Protein Science (1999), *8*:1530–1535. Cambridge University Press. Printed in the USA.

Effects of tryptophan to phenylalanine substitutions on the structure, stability, and enzyme activity of the IIAB^{Man} subunit of the mannose transporter of *Escherichia coli*

ZORA MARKOVIC-HOUSLEY,[1] BEAT STOLZ,[2] REGINA LANZ,[2] AND BERNHARD ERNI[2]

[1]Department of Structural Biology, Biocenter, University of Basel, Klingelbergstrasse 70, CH-4056 Basel, Switzerland
[2]Department of Chemistry and Biochemistry, University of Bern, Freiestrasse 3, CH-3012 Bern, Switzerland

(RECEIVED December 21, 1998; ACCEPTED March 26, 1999)

Abstract

The hydrophilic subunit of the mannose transporter (IIAB^{Man}) of *Escherichia coli* is a homodimer that contains four tryptophans per monomer, three in the N-terminal domain (Trp12, Trp33, and Trp69) and one in the C-terminal domain (Trp182). Single and double Trp-Phe mutants of IIAB^{Man} and of the IIA domain were produced. Fluorescence emission studies revealed that Trp33 and Trp12 are the major fluorescence emitters, Trp69 is strongly quenched in the native protein and Trp182 strongly blue shifted, indicative of a hydrophobic environment. Stabilities of the Trp mutants of dimeric IIA^{Man} and IIAB^{Man} were estimated from midpoints of the GdmHCl-induced unfolding transitions and from the amount of dimers that resisted dissociation by SDS (sodium dodecyl sulfate), respectively. W12F exhibited increased stability, but only 6% of the wild-type phosphotransferase activity, whereas W33F was marginally and W69F significantly destabilized, but fully active. Second site mutations W33F and W69F in the background of the W12F mutation reduced protein stability and suppressed the functional defect of W12F. These results suggest that flexibility is required for the adjustments of protein–protein contacts necessary for the phosphoryltransfer between the phosphorylcarrier protein HPr, IIA^{Man}, IIB^{Man}, and the incoming mannose bound to the transmembrane IIC^{Man}–IID^{Man} complex.

Keywords: bacterial phosphotransferase system; circular dichroism; fluorescence; intragenic suppression

The import of mannose across the plasma membrane of *Escherichia coli* and phosphorylation of the imported sugar are catalyzed by a membrane protein complex of the bacterial phosphoenolpyruvate dependent phosphotransferase system (PTS), which consists of IIC^{Man} and IID^{Man} (transmembrane subunits of the mannose transporter) and IIAB^{Man} (cytoplasmic subunit of the mannose transporter) (Erni & Zanolari, 1985). The PTS mediates the transfer of phosphoryl groups from phosphoenolpyruvate (phosphoryl donor) to carbohydrates and hexitols (phosphoryl acceptor) in the sequence phosphoenolpyruvate → enzyme I → HPr → IIA → IIB-IIC-IID → sugar. Enzyme I (68 kDa), HPr (histidine-containing phosphocarrier protein, 9 kDa), and the IIAB^{Man} subunit of the mannose transporter are transiently phosphorylated on His residues (Meadow et al., 1990; Erni, 1992; Lengeler et al., 1994; Postma et al., 1996). The hydrophilic subunit of the mannose transporter, IIAB^{Man}, is a homodimer (2 × 35 kDa) that can be isolated as soluble protein or in a complex with IIC^{Man} and IID^{Man} (Erni et al., 1987). The IIAB^{Man} dimers are partially resistant to dissociation by SDS (sodium dodecyl sulfate) (Erni & Zanolari, 1985). The IIAB^{Man} monomer is composed of an N-terminal IIA (14 kDa) and a C-terminal IIB domain (20 kDa), which are linked by a flexible hinge. The IIA and IIB domains unfold independently and do not interact significantly with each other (Markovic-Housley et al., 1994). IIA^{Man} and IIB^{Man} become transiently phosphorylated at His10 and His175, respectively (Erni et al., 1989). All four phosphorylation sites in the dimer can be phosphorylated simultaneously, and there is no indication of half-site reactivity (Stolz et al., 1993). The IIA domain has an open pleated α/β fold with four strands forming a parallel β-sheet (strand order 2134), and a fifth antiparallel β-strand originating from an exchange of β-strands 5 between the subunits (Fig. 1) (Nunn et al., 1996). IIB^{Man} also has an α/β fold consisting of a strongly twisted seven-stranded β-sheet with helices on both faces (Schauder et al., 1998). Six Trp → Phe mutants of IIAB^{Man} and IIA^{Man} (W12F, W33F, W69F, W12,33F, W12, 69F, and W33, 69F) were characterized to assess the effect of Trp → Phe substitution on the intrinsic fluorescence, phosphotransferase activity, and protein stability. The results suggest that a certain degree of flexibility of the IIA domain is important for efficient binding and/or phosphoryltransfer between HPr and IIAB^{Man}, and between the IIA and IIB domains within IIAB^{Man}.

Reprint requests to: Bernhard Erni, Department of Chemistry and Biochemistry, University of Bern, Freiestrasse 3, CH-3012 Bern, Switzerland; e-mail: erni@ibc.unibe.ch.

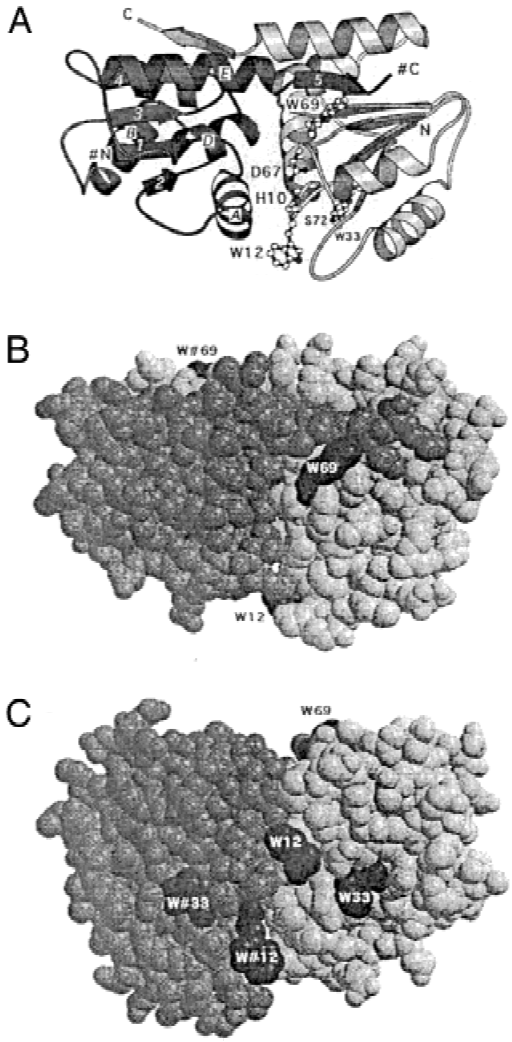

Fig. 1. Structure of the IIA^{Man} dimer (Nunn et al., 1996). **A:** Ribbon diagram. The two subunits are colored black and grey. The four parallel and the one antiparallel β-strand from the opposite subunit are numbered (strand order 21345). Helices A, B, C, D, and E are on both sides of the β-sheet. The side chains of Trp12, Trp33, and Trp69 and the active-site residues His10, Asp67, and Ser72 are indicated. **B:** Space-filling model showing the location of Trp12 and Trp69 in the dimer interface; same view as in **A**. **C:** Space-filling model rotated by 90° around the horizontal axis. Unlike Trp12 and Trp69, Trp33 is not a part of dimer interface.

Results

Fluorescence and far-UV circular dichroism properties

Figure 2 shows the fluorescence emission spectra of wild-type IIAB^{Man} and of its separated domains IIA and IIB (see Table 1). The emission maxima λ_{max} are at 343 nm for IIAB^{Man}, 347 nm for the IIA domain, and 328 nm for the IIB domain. A blue shifted λ_{max} of IIB^{Man} indicates that Trp182 is buried in the hydrophobic interior of the IIB domain. In Figure 2, the fluorescence intensity of the IIB domain (3 μM) is three to four times lower than that of the IIA domain (1 μM) consistent with the presence of one tryptophan (Trp182) in IIB^{Man} and three tryptophans (Trp12, Trp33, and Trp69) in IIA^{Man}. To assess the contribution of the individual Trp to the overall fluorescence intensity of the IIA domain, Trp12,

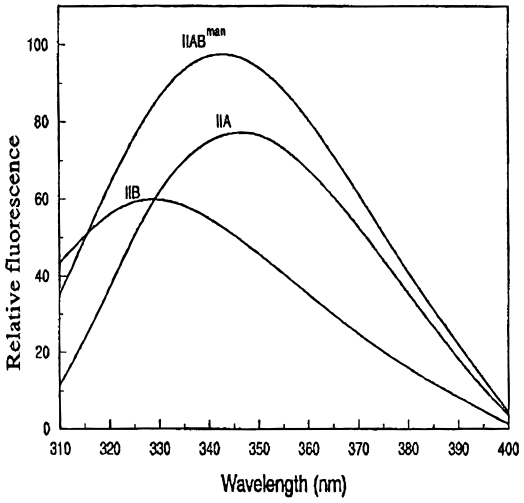

Fig. 2. Fluorescence emission spectra of IIAB^{Man} (1 μM) and its separated domains IIA^{Man} (1 μM) and IIB^{Man} (3 μM). Proteins were dissolved in 20 mM sodium phosphate, pH 7.5. The excitation wavelength was 295 nm.

Trp33, and Trp69 in IIA^{Man} were substituted by Phe, leading to the following single and double mutants: W12F, W33F, W69F, W12,33F, W12,69F, and W33,69F. The emission spectra of the IIA^{Man} wild-type and Trp mutants in their native and denatured states are shown in Figures 3A and 3B, respectively (see Table 1). In native proteins, Trp33 and Trp12 are the major fluorescence emitters in IIA^{Man} since their replacement by Phe decreased the fluorescence intensity by 49 and 37%, respectively, relative to that of the wild-type (Fig. 3A). In contrast, the replacement of Trp69 by Phe lowered the fluorescence intensity by only 7%, indicating that Trp69 was strongly quenched in the wild-type IIA^{Man}. In agreement with this notion, the double mutant W12,33F, which contained only Trp69, had almost zero fluorescence quantum yield in the native state (Fig. 3A). Fluorescence intensity regained the level of the other

Table 1. *Fluorescence emission maxima λ_{max} of IIAB^{Man}, IIA and IIB wild-type, single and double Trp mutants*

Protein	Trp present				λ_{max} (nm) native	denatured
IIAB^{Man} wild-type	12	33	69	182	343	353
IIAB^{Man} W12F	—	33	69	182	337.5	353
IIAB^{Man} W12,69F	—	33	—	182	338	353
IIAB^{Man} W69F	12	33	—	182	344	353
IIAB^{Man} W33,69F	12	—	—	182	343	353
IIAB^{Man} W33F	12	—	69	182	343	353
IIAB^{Man} W12,33F	—	—	69	182	333	353
IIA wild-type	12	33	69		347	353
IIA W12F	—	33	69		341	353
IIA W12,69F	—	33	—		341	353
IIA W69F	12	33	—		348	353
IIA W33,69F	12	—	—		351.5	353
IIA W33F	12	—	69		351	353
IIA W12,33F	—	—	69		n.d.[a]	353
IIB wild-type				182	328	353

[a] n.d., not detected.

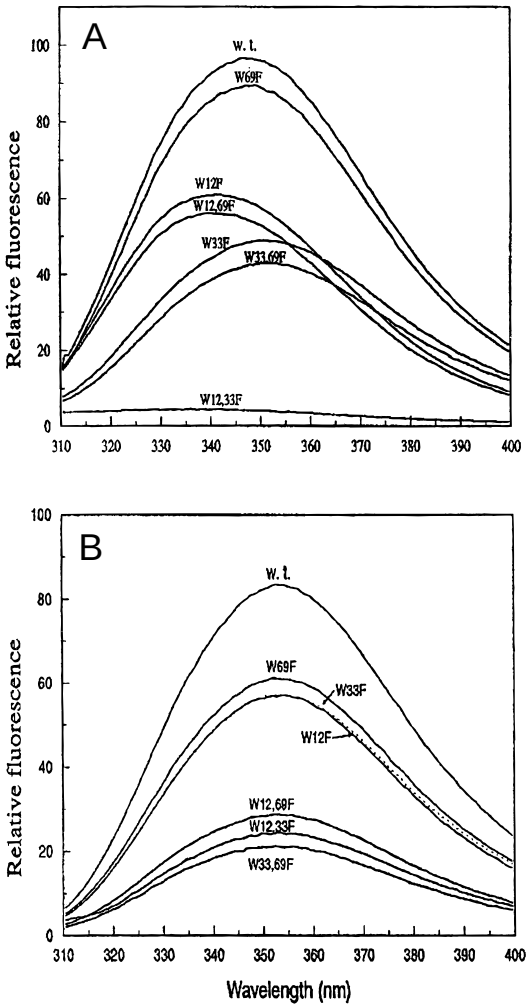

Fig. 3. Fluorescence emission spectra (excitation at 295 nm) of the wild-type IIA domain and six Trp mutants. **A:** Native proteins in 20 mM sodium phosphate, pH 7.5. **B:** Denatured proteins in 6 M GdmHCl. Protein concentration was 1.5 μM in all cases.

single Trp mutants upon denaturation in 6 M GdmHCl (Fig. 3B). The fluorescence intensities of the Trp mutants denatured in 6 M GdmHCl were proportional to the Trp content, approximately two-thirds for the single substitution and one-third for the double substitution mutants. Solvent exposure of individual Trp in IIA^{Man} was estimated from the positions of the maxima in the emission spectra λ_{max} (see Table 1). Trp12 is near the protein surface since λ_{max} of the W33,69F mutant (containing only Trp12) is red shifted to 352 nm, while the removal of Trp12 (W12F) causes a 6 nm blue shift of λ_{max}. Trp33 appears to be slightly shielded from the solvent because λ_{max} of the single Trp33 (W12,69F mutant) is at 341 nm, while the λ_{max} of W33F is 4 nm red shifted relative to a wild-type. The low fluorescence intensity of the W12,33F mutant, which contains a single Trp69, prevented an accurate estimate of λ_{max} for Trp69. Spectral characteristics of the wild-type $IIAB^{Man}$ and its Trp mutants (data not shown) were qualitatively similar to those of IIA^{Man} and are summarized in Table 1.

The overall shape and amplitudes of far-ultraviolet (UV) circular dichroism (CD) spectra (250–190 nm) of all mutants were similar to that of the wild-type $IIAB^{Man}$ (data not shown) indicating that no global changes of the secondary structure were induced by replacing selected Trp by Phe.

Phosphotransferase activity of $IIAB^{Man}$ mutants

The ability of Trp mutants of $IIAB^{Man}$ to restore mannose transport and phosphorylation gave similar results in vivo and in vitro. In vivo, the transformants expressing the W12F mutant formed yellow colonies, suggesting that the substitution of Trp12 by Phe impaired the function of $IIAB^{Man}$. All other transformants expressing single and double mutants formed dark red colonies as did the wild-type cells. The purified W12F protein had only 6% of the wild-type activity in the phosphotransferase assay whereas all other Trp mutants exhibited activities similar to wild-type $IIAB^{Man}$. However, the defect of W12F mutant could be reversed when in addition to Trp12 either Trp69 or Trp33 was also replaced by Phe. While the low activity of W12F mutant is not surprisingly given the proximity of Trp12 to the transiently phosphorylated His10, the restoration of W12F activity to wild-type level by a second mutation of either Trp33 or Trp69 was unexpected.

Stability of the Trp mutants of IIA^{Man} and $IIAB^{Man}$ to denaturants

To correlate the functional differences among Trp mutants to their physical properties, the stability of each mutant of $IIAB^{Man}$ and IIA^{Man} against denaturation by SDS and GdmHCl, respectively, was measured. Wild-type $IIAB^{Man}$ and the IIA domain are homodimers and the treatment with denaturants will cause polypeptide unfolding with concomitant dissociation of the dimers. The stabilities of the IIA mutants were determined from the midpoints of the GdmHCl-induced equilibrium unfolding transitions (C_m), which were monitored by the intrinsic fluorescence at λ_{max}. All transitions were monophasic and reversible, similar to that reported for wild-type IIA^{Man} (Markovic-Housley et al., 1994). The unfolding transitions of four Trp mutants (6 μM), which differ mostly from the wild-type, are shown in Figure 4. Replacement of Trp12 by Phe stabilizes the IIA domain, whereas substitution of Trp69 by Phe has a destabilizing effect, as shown by the shifts of the midpoint transitions by +0.3 M and −0.2 M GdmHCl, and the calculated $\Delta\Delta G^{\circ}(H_2O)$ of −15 and 18 kJ mol^{-1}, respectively, relative to the wild-type (2.3 M GdmHCl; $\Delta G^{\circ}(H_2O)$ 44 ± 11 kJ mol^{-1}) (Table 2). The W33F and W69F mutants are less stable than the wild-type. When either of the two mutations (W33F or W69F) is introduced into the W12F background, the stability of the double mutant is restored to near wild-type level of $\Delta G^{\circ}(H_2O)$ 45 ± 7 kJ mol^{-1}. Differences in stabilities were also seen when the resistance of the Trp mutants to dissociation by low concentration of SDS (0.05%) was tested by SDS-polyacrylamide gel electrophoresis (Fig. 5). $IIAB^{Man}$ dimers dissociate only partially under these conditions and the effect of different mutations on the dimer stability can be directly estimated from the monomer to dimer ratios in stained polyacrylamide gels. Of the wild-type $IIAB^{Man}$ 20% remained dimeric and of W33F 16% remained dimeric. The W69F mutant and the double mutants lacking Trp69 were completely dissociated (Fig. 5; Table 2) suggesting that Trp69 plays a particular role in stabilizing the $IIAB^{Man}$ dimer. In contrast, the W12F mutant was 50% resistant to dissociation by SDS and replacement of Trp12 also resulted in an increased stability of the W12,33F but not of the W12,69F double mutant. The latter mutant, which contains only Trp33, is fully dissociated by SDS.

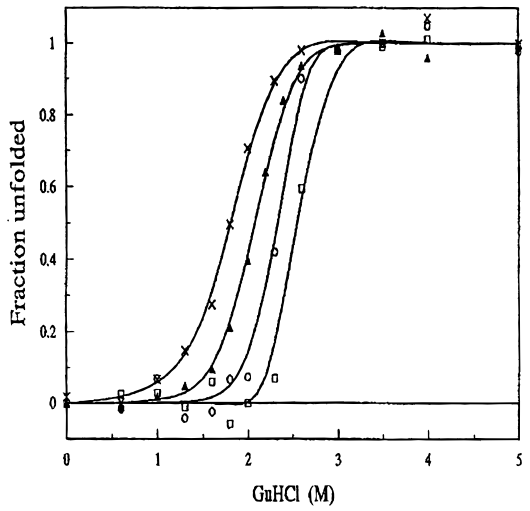

Fig. 4. GdmHCl-induced unfolding of IIA^{Man} wild-type (open circles) and the selected Trp mutants: W12F (open squares); W69F (solid triangles); and W33,69F (stars), monitored by fluorescence emission at λ_{max}. Protein concentration was 6 μM. Normalized data are reported as the fraction of the unfolded protein. All data were normalized to the difference between the linear changes observed above and below transition region. Solid lines are the smoothed curves drawn through the data points.

Discussion

$IIAB^{Man}$ is the energy-coupling subunit of the mannose transporter. It consists of two independently folding protein domains (IIA and IIB). $IIAB^{Man}$ forms tight homodimers that are stabilized by hydrophobic contacts and the reciprocal exchange of one β-strand between the five-stranded β-sheets of the IIA domains. The IIB domains reversibly bind to the IIC^{Man}–IID^{Man} complex. $IIAB^{Man}$ activates sugar translocation and mediates phosphoryltransfer between the phosphorylcarrier protein HPr and the transported sugar. Here we characterize the effects of three Trp to Phe substitutions on the activity and stability of the $IIAB^{Man}$ subunit.

$IIAB^{Man}$ of *E. coli* contains four Trp, three in the IIA and one in the IIB domain. Trp12 and Trp69 both are located in the dimer interface between the IIA domains. Trp12 interacts across the dimer interface with Gln16, Lys19, and Met23 from helix A of the opposite subunit. The side chain of Trp69 is closely packed ($<$4 Å) against Lys127, Ala128, and Leu129 of the antiparallel β-strand 5 from the other subunit (Fig. 1). Trp33 is far from the dimer interface, and Trp182 is buried in the interior of the IIB domain (Nunn et al., 1996; Schauder et al., 1998).

The fluorescence of Trp69 is quenched relative to the other Trp as indicated by the facts that exchange of Trp69 for Phe hardly affected the fluorescence spectra of the $IIAB^{Man}$ and that the fluorescence intensity of wild-type $IIAB^{Man}$ increased upon denaturation. This quenching of Trp69 may be due to a proximate charged amino acid residue (Beechem & Brand, 1985) or to energy transfer to another Trp. We favor the former interpretation for two reasons: (1) Trp69 is closely packed against Lys127, in β-strand 5 from the other subunit, which may act as a quencher. Upon unfolding with GdmHCl the dimer interface is broken and the quenching of the fluorescence abolished. (2) The fluorescence emission of Trp69 does not increase significantly in the mutants lacking Trp12 or Trp33. Fluorescence data indicate that Trp12 is highly exposed and Trp33 is partially shielded, while the exposure of Trp69 could not be determined due to low fluorescence intensity. In the crystal structure of IIA^{Man} (Nunn et al., 1996), the solvent accessible surface area is 110 $Å^2$ for Trp12 and Trp69 and 180 $Å^2$ for Trp33, calculated according to Lee and Richards (1971). The fluorescence of Trp182 is blue shifted in agreement with the buried position and a solvent accessible surface area of only 6.5 $Å^2$.

Trp12 and Trp69 are near the invariant active-site residues His10 and Asp67 (catalytic diade) in loops 1/A and 3/C of the topological switch point of the α/β fold. Trp33 is far from the active-site. Trp182 is in the amino acid sequence near the active-site His175 of the IIB domain. Of the four Trp, Trp182 is invariant in all four homologous sequences listed in the EMBL/SwissProt database and in 25 out of 26 additional homologous sequences, which could be found in bacterial genomes (complete and in progress; http://www.ncbi.nlm.nih.gov/BLAST/unfinishedgenome.html). In contrast, Trp69 was conserved only five times and Trp33 only once. In spite of its close proximity to the active-site His10, Trp12 is not conserved in any of the homologous sequences. Instead, polar and bulky hydrophilic groups such as Arg, Lys, Gln, His, Asn, and Asp are found. Therefore no strong effects upon structure and catalytic activity would have been expected from the substitutions by Phe of the Trp in the IIA domain. Indeed, none of six mutant proteins (W12F, W33F, W69F, W12,33F, W12,69F, and W33,69F) showed significant alterations in the native structure as judged by far-UV CD spectra, which were essentially identical to that of the wild-type protein. Substitution of the least conserved Trp12 had the strongest effect upon phosphotransferase activity, which was reduced to 6% of the wild-type control, whereas the stability against SDS and GdmHCl induced unfolding was increased (Table 2). Substitutions of Trp33 and Trp69 by Phe did not affect activity but resulted in a decrease of stability against SDS and GdmHCl induced unfolding. Surprisingly, the effects on activity and stability of the W12F substitution were completely reversed by either the W33F or W69F second site mutation. W12,33F and W12,69F double mutants displayed close to 100% activity and wild-type stability. Even the W12,33,69F/S110C quadruple mutant retained 90% of activity relative to the S110C single mutant (Stolz et al., 1993; Hochuli, 1996).

In conclusion, phosphotransferase activity and stability of $IIAB^{Man}$ are inversely related. The increased stability of the W12F mutant compromises catalytic activity and this effect can be reversed by destabilizing second site mutations. Too "rigid" a structure might prevent conformational adjustments in IIA^{Man} necessary for the binding of the structurally different proteins HPr and IIB^{Man}, and for the transfer of the phosphoryl groups between their active sites. The fact that the mutants, which are less stable than the wild-type, are fully active supports the notion that flexibility must be an important prerequisite for activity of the $IIAB^{Man}$ subunit. Trp33 and Trp69 are at approximately 7 and 23 Å edge to edge distance from Trp12, such that a direct interaction between these residues is not possible. The environments of Trp12, Trp33, and Trp69 are quite different. Trp12 in loop 1/A interact across the dimer interface with Gln16, Lys19, and Met23 of helix A of the opposite subunits. Thirty-two percent of their total surface areas are buried in the dimer interface. Trp69 in loop 3/C are closely packed ($<$4 $Å^2$) against Lys127, Ala128, and Leu129 of the antiparallel β-strands 5 from the other subunits with 44% of their surface area buried in the dimer interface. Trp33 are completely surrounded by residues of their own subunits. Whereas the W69F mutation could weaken the interaction of the subunits in the dimer, it is not clear from the structure which kind of change may occur

Table 2. *Phosphotransferase activity and stability against GdmHCl and SDS denaturation of IIA^{Man} and IIAB^{Man} mutants*

Protein	Phosphotransferase activity (% of wild-type)	Stability of IIA^{Man}		SDS stability of IIAB^{Man} (% dimer)
		C_m (M GdmHCl)	$\Delta G°(H_2O)$ (kJ mol^{-1})	
IIAB^{Man} wild-type	100	2.3	44 ± 11	20
IIAB^{Man} W12F	6	2.6	59 ± 15	50
IIAB^{Man} W33F	113	2.2	35 ± 6	16
IIAB^{Man} W69F	111	2.1	26 ± 3	0
IIAB^{Man} W12,33F	93	2.2	45 ± 7	29
IIAB^{Man} W12,69F	103	2.1	46 ± 5	0
IIAB^{Man} W33,69F	98	1.8	22 ± 4	0

in the W12,33F mutant that could account for the observed compensating effect. There is no evidence from the X-ray structure that Trp12 adds conformational strain, which would be relaxed by substitution with a residue of reduced side-chain volume. It is, however, possible that any mutation leading to a reduced stability, and consequently increased flexibility, could have counteracted the stabilizing effect of the W12F substitution and thereby suppressed the functional defect.

Materials and methods

Protein expression and purification

Trp mutants of IIAB^{Man} were constructed in phagemid vectors using the gapped duplex technique (Stanssens et al., 1989; Stolz et al., 1993). The Trp mutants were overexpressed in *E. coli* strain WA2127ΔHIC and purified by phosphocellulose and gelfiltration chromatography (Stolz et al., 1993). Limited tryptic digestion of IIAB^{Man} (at a molar ratio IIAB^{Man}: trypsin between 400:1 to 1,000:1) was used to produce the N-terminal IIA and the C-terminal IIB domains, which were separated on phosphocellulose and further purified by gel filtration chromatography. Protein concentrations were determined from the optical density at 280 nm (Gill & von Hippel, 1989). Calculated extinction coefficients were: 29,365, 19,630, and 9,530 M^{-1} cm^{-1} for the wild-type IIAB^{Man}, IIA^{Man}, and IIB^{Man}, respectively; 23,470 M^{-1} cm^{-1} for the single mutants (W12F, W33F, and W69F) and 17,780 M^{-1} cm^{-1} for the double mutants (W12,33F, W12,69F, and W33,69F) of IIAB^{Man}; 13,940 M^{-1} cm^{-1} for the single mutants (W12F, W33F, and W69F) and 8,250 M^{-1} cm^{-1} for the double mutants (W12,33F, W12,69F, and W33,69F) of IIA^{Man}.

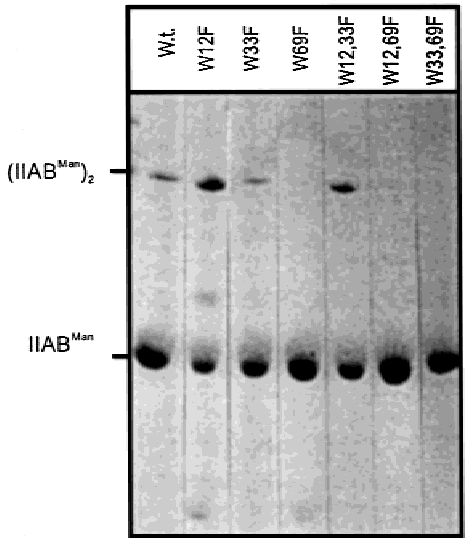

Fig. 5. SDS-polyacrylamide gel electrophoresis of the IIAB^{Man} wild-type and its Trp mutants. The positions of the IIAB^{Man} monomers (35 kDa) and dimers (70 kDa) are indicated on the right side, and the molecular masses of marker proteins in kDa on the left.

Spectroscopic studies

Samples were dissolved in 20 mM sodium-phosphate, pH 7.4 for all experiments. High purity GdmHCl (guanidinium hydrochloride) was purchased from Sigma (St. Louis, Missouri). The intrinsic fluorescence spectra of wild-type and mutant proteins were measured on a LS-5B Perkin-Elmer (Foster City, California) spectrofluorometer using a 5 mm light-path cell. Excitation and emission bandwidths were set at 7 and 10 nm, respectively. Emission spectra (295 nm excitation) of native and denatured proteins were recorded with solutions of identical protein concentrations. This was achieved by equal dilution of the concentrated protein solution with either 20 mM sodium phosphate, pH 7.4, or with 8 M GdmHCl in 20 mM sodium phosphate, pH 7.4. The final protein concentrations were between 1 and 3 μM. All spectra were corrected for solvent emission. The far-UV CD spectra were recorded on a Jasco spectropolarimeter (J500-A) using a 0.5 mm light-path cell (Markovic-Housley et al., 1994).

Fluorescence intensity was used to follow GdmHCl-induced unfolding. Protein samples were equilibrated with GdmHCl-containing buffers for 2 h at 22 °C before the measurements. For refolding studies, protein samples were first fully denatured in 8 M GdmHCl for 2 h at 22 °C and subsequently diluted to lower final concentrations of GdmHCl. The unfolding reaction was fully reversible for all Trp mutants of IIA^{Man}. Protein concentration was 6.0 μM. Transition curves are presented as the fraction of unfolded protein, f_u vs. GdmHCl concentration. f_u was calculated from the experimental data by using the equation: $f_u = (y_f - y_{obs})/(y_f - y_u)$, where y_{obs} is the observed variable parameter (fluorescence emission), and y_f and y_u are parameters characteristic of the folded and un-

folded state. Values of f_u in the transition region were calculated by extrapolating the linear portions of the pre- and post-transitional regions of the unfolding curve into the transition region (Markovic-Housley et al., 1994). $\Delta G^\circ(H_2O)$ were determined from the non-linear least-squares fit of the equation:

$$y_{obs} = a * [\text{GdmHCl}] + b + \frac{c * [\text{GdmHCl}] + d - a * [\text{GdmHCl}] - b}{1 + \exp((\Delta G^\circ - k * [\text{GdmHCl}])/RT)}. \quad (1)$$

Electrophoresis

Polyacrylamide gel electrophoresis in the presence of SDS was used to assess the stability of the $IIAB^{Man}$ dimers against dissociation by SDS. The $IIAB^{Man}$ mutants proteins were incubated in sample buffer containing 0.1% SDS for 20 min at room temperature and then separated on a 15% polyacrylamide gel containing 0.1% SDS. The dimer to monomer ratio was determined from the densitometric scans of the Coomassie blue stained gel.

Assay for phosphotransferase activity

The phosphotransferase activity of $IIAB^{Man}$ and its Trp mutants were tested in vivo by using the *E. coli* WA2127 containing plasmid pTSPM6, which encodes the transmembrane subunits IIC^{Man} and IID^{Man} (Erni et al., 1989). Transformants expressing the different mutants were placed on McConkey mannose indicator plates and colonies were classified for their fermentation phenotype. The wild-type cells and transformants expressing the active Trp mutants formed red colonies while the mutants with impaired activity formed yellow colonies. The in vitro phosphotransferase activity of the purified $IIAB^{Man}$ mutants was assayed in the presence of enzyme I, HPr, a membrane fraction containing IIC^{Man} and IID^{Man}, phosphoenolpyruvate, and [^{14}C]glucose (Stolz et al., 1993).

Acknowledgments

We thank Ms. Karin Flükiger for excellent technical assistance and Dr. T. Schirmer for stimulating discussions and providing Figure 1. This work was supported by Grant 31-45838.95 from the Swiss National Science Foundation.

References

Beechem JM, Brand L. 1985. Time-resolved fluorescence of proteins. *Annu Rev Biochem 54*:43–71.

Erni B. 1992. Group translocation of glucose and other carbohydrates by the bacterial phosphotransferase system. *Int Rev Cytol 137A*:127–148.

Erni B, Zanolari B. 1985. The mannose-permease of the bacterial phosphotransferase system. Gene cloning and purification of the Enzyme II^{Man}/III^{Man} complex of *Escherichia coli*. *J Biol Chem 260*:15495–15503.

Erni B, Zanolari B, Graff P, Kocher HP. 1989. Mannose permease of *E. coli*. Domain structure and function of the phosphorylating subunit. *J Biol Chem 264*:18733–18741.

Erni B, Zanolari B, Kocher HP. 1987. The mannose permease of *E. coli* consists of three different proteins: Amino acid sequence and function in sugar transport, sugar phosphorylation, and penetration of phage lambda DNA. *J Biol Chem 262*:5238–5247.

Gill SC, von Hippel PH. 1989. Calculation of protein extinction coefficients from amino acid sequence data. *Anal Biochem 182*:319–326.

Hochuli M. 1996. The mannose transporter of *E. coli*: Monitoring conformational changes in the IIAB subunit by fluorescence spectroscopy [Diploma thesis]. Bern, Switzerland: University of Bern.

Lee B, Richards FM. 1971. The interpretation of protein structures: Estimation of static accessibility. *J Mol Biol 55*:379–400.

Lengeler JW, Jahreis K, Wehmeier UF. 1994. Enzymes II of the phosphoenolpyruvate-dependent phosphotransferase systems: Their structure and function in carbohydrate transport. *Biochim Biophys Acta 1188*:1–28.

Markovic-Housley Z, Cooper A, Lustig A, Flükiger K, Stolz B, Erni B. 1994. Independent folding of the domains in the hydrophilic subunit $IIAB^{Man}$ of the mannose transporter of *E. coli*. *Biochemistry 33*:10977–10984.

Meadow ND, Fox DK, Roseman S. 1990. The bacterial phosphoenolpyruvate: Glycose phosphotransferase system. *Annu Rev Biochem 59*:497–542.

Nunn RS, Markovic-Housley Z, Génovésio-Taverne JC, Flükiger K, Rizkallah PJ, Jansonius JN, Schirmer T, Erni B. 1996. Structure of the IIA domain of the mannose transporter from *E. coli* at 1.7 Å resolution. *J Mol Biol 259*:502–511.

Postma PW, Lengeler JW, Jacobson GR. 1996. Phosphoenolpyruvate:carbohydrate phosphotransferase systems. In: Neidhardt FC, Curtiss R, Ingraham JL, Lin ECC, Low KB, Magasanik B, Reznikoff WS, Riley M, Schaechter M, Umbarger HE, eds. *Escherichia coli and Salmonella typhimurium: Cellular and molecular biology*. Washington, DC: ASM Press. pp 1149–1174.

Schauder S, Nunn RS, Lanz R, Erni B, Schirmer T. 1998. Crystal structure of the IIB subunit of the fructose permease from *Bacillus subtilis*. *J Mol Biol 276*:591–602.

Stanssens P, Opsomer C, McKeown YM, Kramer W, Zabeau M, Fritz HJ. 1989. Efficient oligonucleotide-directed construction of mutations in expression vectors by the gapped duplex DNA method using alternating selectable markers. *Nucleic Acids Res 17*:4441–4445.

Stolz B, Huber M, Markovic-Housley Z, Erni B. 1993. The mannose transporter of *E. coli*—Structure and function of the $IIAB^{Man}$ subunit. *J Biol Chem 268*:27094–27099.